Facile synthesis of nanorod-assembled multi-shelled Co_3O_4 hollow microspheres for high-performance supercapacitors

CrossMark

Yaping Wang [a], Anqiang Pan [a, *], Qinyu Zhu [a], Zhiwei Nie [a], Yifang Zhang [a], Yan Tang [a], Shuquan Liang [a, *], Guozhong Cao [b, *]

[a] School of Materials Science & Engineering, Central South University, Hunan 410083, China
[b] Department of Materials Science & Engineering, University of Washington, Seattle, WA 98195, USA

HIGHLIGHTS

- Nanorod-assembled cobalt precursor has been successfully grown on the surface of carbon microspheres.
- Multi-shelled interior structures within the microspheres are created during the carbon microspheres removal process.
- The as-prepared multi-shelled Co_3O_4 hollow microspheres exhibit excellent rate capability for supercapacitors.

GRAPHICAL ABSTRACT
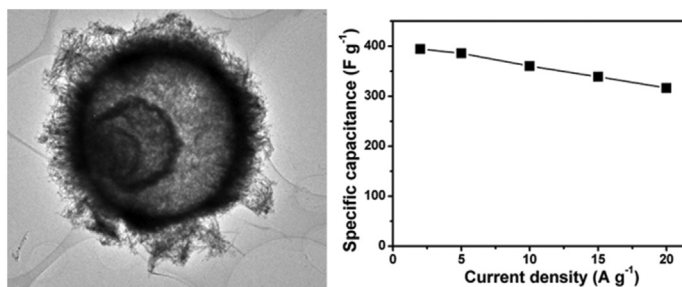
ARTICLE INFO

ABSTRACT

In this work, we report a novel strategy for the controlled synthesis of nanorod assembled multi-shelled cobalt oxide (Co_3O_4) hollow microspheres (HSs). The $Co_2CO_3(OH)_2$ NRs are first vertically grown on the carbon microspheres (CS) to form the core-shelled composites by a low-temperature solution route. The multi-shelled hollow interiors within the Co_3O_4 microspheres are unconventionally obtained by annealing the as-prepared core–shell structured CS@$Co_2CO_3(OH)_2$ composite in air. When evaluated for supercapacitive performance, the multi-shelled Co_3O_4 hollow microspheres exhibit high capacitance of 394.4 and 360 F g^{-1} at the current densities of 2 A g^{-1} and 10 A g^{-1}, respectively. The superior electrochemical performance can be attributed to the multi-shelled hollow structures, which facilitate the electrolyte penetration and provide more active sites for the electrochemical reactions.

1. Introduction

Hollow micro-/nanostructures with controllable complex structures have attracted extensive attention in recent years because of their promising properties in many fields, such as drug delivery [1,2], gas sensors [3,4] and energy storage and conversion [5,6]. In particular, the complex hollow structures such as multi-shelled hollow structures and yolk-shelled structures have stimulated researchers' great interest, as these complex structures can offer new avenues to tailor the properties for different applications [7–9]. Although template-free routes have been more frequently reported for the preparation of hollow particles [9–11], templating against colloidal particles is still the most effective and general method for the preparation of hollow particles with controllable size distribution and morphology [12,13]. Monodisperse polymer

* Corresponding authors.
    E-mail addresses: pananqiang@csu.edu.cn (A. Pan), lsq@mail.csu.edu.cn (S. Liang), gzcao@u.washington.edu (G. Cao).

latex [14,15], carbon [16,17] and silica spheres are the common hard colloidal templates [8] owing to their availability in a wide range of sizes. The two issues should be addressed before obtaining hollow structured materials with high quality: 1) the uniform coating of desired materials (or their precursors) on the surface of templates and 2) the maintenances of their structural integrities after removing templates. Moreover, constructing hollow particles with complex architectures, such as multi-shell or yolk-shell structures by a simple templating process still remains a big challenge.

Cobalt oxide (Co_3O_4) is selected for study because of its high theoretical capacity, good chemical and thermal stability, and low cost as compared to the state-of-the-art supercapacitor materials, such as ruthenium dioxide [18–20]. However, their large applications are limited by their fairly low electronic conductivity and large volume changes during the redox reaction process. Recently, porous and hollow structured Co_3O_4 materials have drawn particular interest in energy storage applications because of their structural advantages for facile ions transportation and good cycling stability [18,21]. Template-free strategies have been more commonly employed for the synthesis of Co_3O_4 hollow microspheres. It is still a big challenge to accurate control their interior structures, in particular for the construction of complex interior structures. Templating against colloidal particles usually get uniform Co_3O_4 hollow structures, but the as-prepared structures are usually of a single shell [22,23]. More recently, Wang and his co-workers reported the accurate synthesis of multishelled Co_3O_4 hollow microspheres using carbonaceous microspheres as sacrificial templates by controlling the size and diffusion rate of the hydrated metal cations and the ion-absorption capability of carbon microspheres [24]. The as-prepared multi-shelled microspheres are all of smooth surface, but no further work is reported on the engineering the exterior shell structures. It is expected the volumetric energy density of the multi-shelled Co_3O_4 is higher than the single-shell structured Co_3O_4 microspheres, because of the further usage of the empty space within the hollow microspheres. Therefore, it would be interesting to obtain hollow microspheres with both complex exterior and interior structures.

Herein, we report the success formation of nanorod-assembled, multi-shelled Co_3O_4 hollow microspheres by first fabricating the carbon microspheres@$Co_2CO_3(OH)_2$ (CS@Co–P) core–shell composite microspheres, with a subsequent calcination process. The resulting rattle-type Co_3O_4 hollow microspheres exhibit a high specific capacitance of 394 F g^{-1} at the current density of 2 A g^{-1}, with good rate capability and high specific capacitance.

2. Experimental section

2.1. Materials synthesis

All the solvents and chemicals were of reagent grade and used without further purification. The cobalt nitrate hexahydrate and urea were obtained from Shanghai Chemical Reagent Co. The carbon spheres were hydrothermally synthesized according to the method in an early report [25]. To prepare the CS@Co–P core–shell composite, 50 mg of carbon spheres were dispersed into 100 mL of the mixed solvent of water and alcohol (1:1, v/v) by ultrasonification. Then 1 g of urea and 200 mg of $Co(NO_3)_2 \cdot 6H_2O$ were dissolved successively to get the mixture solution, which was heated in an oil bath at 80 °C under magnetically stirring for 12 h. The as-obtained materials were collected by centrifugation and washed several times by water and alcohol for several times, followed by drying in air at 60 °C for 12 h. The hierarchical multi-shelled Co_3O_4 hollow microspheres can be obtained after annealing the core-shelled CS@Co–P composite in air at 500 °C for 2 h with a heating ramp rate of 3 °C min^{-1}.

2.2. Structural characterization

The crystal structure of the products was determined by powder X-ray diffraction (XRD, Rigaku D/max2500) using Cu Kα radiation ($\lambda = 1.54178$ Å). The samples were scanned in the range between 10° and 80° (2θ) with a step size of 0.02°. The morphologies and structures of the samples were observed by scanning electron microscopy (SEM, FEI Nova NanoSEM 230) and transmission electron microscopy (TEM, JEOL JEM-2100F). The calcination process in air was studied by thermogravimetric analysis (TGA) and differential scanning calorimetry (DSC) using a heating rate of 10 °C min^{-1}.

2.3. Electrochemical measurements

The multi-shelled Co_3O_4 hollow microspheres, acetylene black and polyvinylidene fluoride (PVDF) in a weight ratio of 80:10:10 were dispersed in an N-methyl-2-pyrrolidone (NMP) solution to make a slurry which was coated on a piece of clean Ni foam substrate with 1×2 cm^2 in size and dried in a vacuum oven at 90 °C for 12 h. The mass loading is about 1 mg cm^{-2}. The electrochemical measurements were carried out in a three-electrode system with a Pt foil counter electrode and an Hg/HgCl reference electrode in 2 M KOH aqueous solution as the electrolyte. Cyclic voltammetry (CV) measurements were performed on an electrochemical workstation (CHI660C, Shanghai) at various scan rates in the voltage range of 0–0.5 V. The constant current charge–discharge was tested at different current densities. The specific capacitances were calculated according to the charge/discharge test and the following equation:

$$C = \frac{I\Delta t}{M\Delta V} \qquad (1)$$

where C (F g^{-1}) is the specific capacitance, I (A) represented the discharge current, Δt (s) is the discharging time, ΔV (V) is the voltage window, and M (g) is the mass of active materials.

3. Results and discussions

The colloidal carbon spheres were first prepared by a hydrothermal method using glucose as the carbon source. As shown in Fig. 1, the carbon spheres are uniform with a mean size of ~1.5 μm. Because of the large amount of hydrophilic functional groups on the
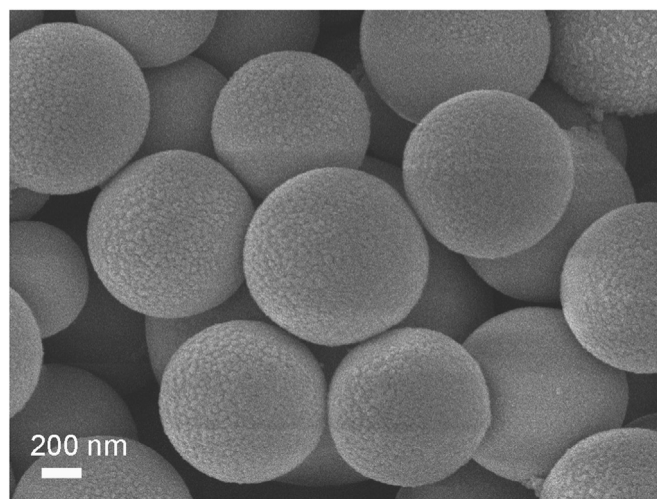

Fig. 1. FESEM images of the carbon microspheres fabricated by hydrothermal method using glucose as carbon precursor.

surface and the easy removal *via* calcinations, these carbon spheres are very attractive as hard templates for the fabrication of hollow particles [25,26]. The synthesis of the core−shell structured carbon spheres@$Co_2CO_3(OH)_2$ composite spheres and their translation into multi-shelled Co_3O_4 hierarchical hollow microspheres are schematically illustrated in Fig. 2. As indicated by step I in Fig. 2, the cobalt precursor nanorods are self-assembled on the carbon spheres during the hydrothermal process to form the core−shell CS@Co−P composite microspheres. After annealing the CS@Co−P microsphere composite in air (step II), the multi-shelled Co_3O_4 hollow microspheres with vertically grown nanorods can be obtained. The structure of the exterior shell remains intact after calcinations in air. Moreover, the multi-shells within the microspheres can be interestingly created during this process. The powder X-ray diffraction (XRD) patterns of the as-prepared precursor and its calcination product are shown in Fig. 3a. The identified diffraction peaks of the precursor can be assigned to monoclinic $Co_2CO_3(OH)_2$ (JCPDS no.48-0083) [27]. The formation of $Co_2CO_3(OH)_2$ can be attributed to the reaction from Co^{2+}, and CO_3^{2-} and OH^- from the hydrolysis of urea. After calcinations at 500 °C for 2 h, the phase pure Co_3O_4 (Fig. 3a) can be obtained, where all the identified peaks can be assigned to the face centered Co_3O_4 (JCPDS file no. 43-1003, space group: $Fd3m(227)$) [4]. The phase transitions from CS@Co−P precursor composite to Co_3O_4 hollow microspheres were investigated by TGA and DSC, and the results are shown in Fig. 3b. The initial weight loss below 220 °C can be mainly attributed to the evaporation of physical adsorbed water. With the increasing of temperatures, the fast weight drop and the corresponding broad exothermic peak between 300 °C and 400 °C on the DSC curve have been detected, which is related to the decomposition of $Co_2CO_3(OH)_2$ and the removal of carbon spheres. A flat plateau after 400 °C on the TGA curve is observed, indicating the complete removal of carbon spheres and the conversion of $Co_2CO_3(OH)_2$ into Co_3O_4.

The morphology and the assembled structures of the CS@Co−P composites were investigated by FESEM and TEM techniques, and the results are shown in Fig. 4. As shown in Fig. 4a, the surface of the carbon microsphere templates are homogeneously covered by $Co_2CO_3(OH)_2$ NRs to form the uniform core−shell structured CS@Co−P composite. The high efficiency of growing cobalt precursor nanorods on the surface of carbon microspheres can be attributed to the existence of large amount of functional groups on the carbon spheres. The TEM image (Fig. 4c) shows the spherical morphology of the CS@Co−P composite, the surface of which is homogeneously covered by cobalt precursor nanorods. The difficulty of detecting carbon microsphere 'core' can be attributed to the dense stacking of nanorods on carbon microspheres. Fig. 4d demonstrates that the $Co_2CO_3(OH)_2$ precursor nanorods in a diameter of less than 20 nm can grow over 500 nm in length.

The nanorod-assembled multi-shelled Co_3O_4 hollow microspheres can be obtained after calcination in air at 500 °C for 2 h. According to the FESEM images (Fig. 5a, b), the nanorod-assembled exterior shell structures can be well preserved after annealing in
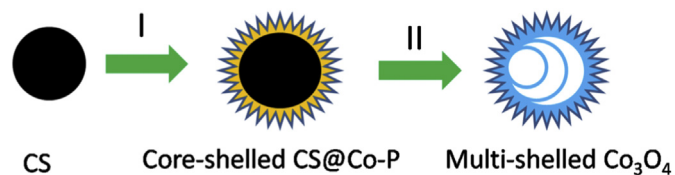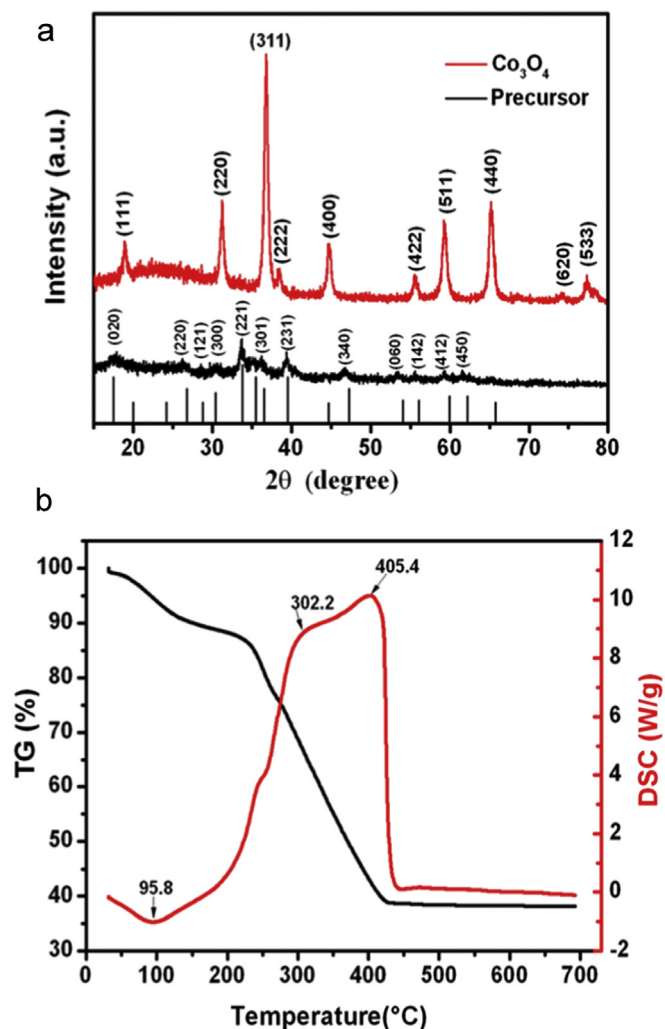

Fig. 3. (a) XRD patterns of the precursor (black) and its annealed product (red); (b) TG and DSC results for the precursor. The temperature ramp rate was 10 °C min^{-1}. (For interpretation of the references to color in this figure legend, the reader is referred to the web version of this article.)

Fig. 2. Schematic illustration of the preparation of core-shelled carbon microspheres@cobalt precursor (CS@Co−P) (step I) and their conversion to the multi-shelled Co_3O_4 hollow spheres (step II).

air. A broken microsphere reveals the hollow interior and the smaller spheres inside the microsphere, indicating the ball-in-ball structures (Fig. 5b). The interior structures of the Co_3O_4 microspheres are further studied by TEM. The low magnification TEM image (Fig. 5c) demonstrates the multi-shell interior structures within the microspheres, corresponding well with the FESEM result in Fig. 5b. The typical TEM image of a single microsphere is shown in Fig. 5d. Triple shells including an exterior shell and two interior shells are clearly detected for the hollow microspheres. The diameters of the triple shells are about 1.8, 1.0 and 0.5 μm, respectively. Moreover, large space between the neighboring shells is clearly exhibited. Generally, removing the hard template from a simple core−shell structure usually produce single-shelled hollow particles [6]. The formation of multi-shell hollow structures from a simple hard templating process in the present work is therefore considered quite unusual. We postulate the formation mechanism as follows: The cobalt species are strongly bonded to the surface of the carbon spheres because of the existence of abundant functional groups. During the calcination process, the outer layer of cobalt precursor crystallizes into the rigid Co_3O_4 outer shell, which is similar to typical template-assisted formation of hollow structures. It is believed the concentration of cobalt species within the carbon
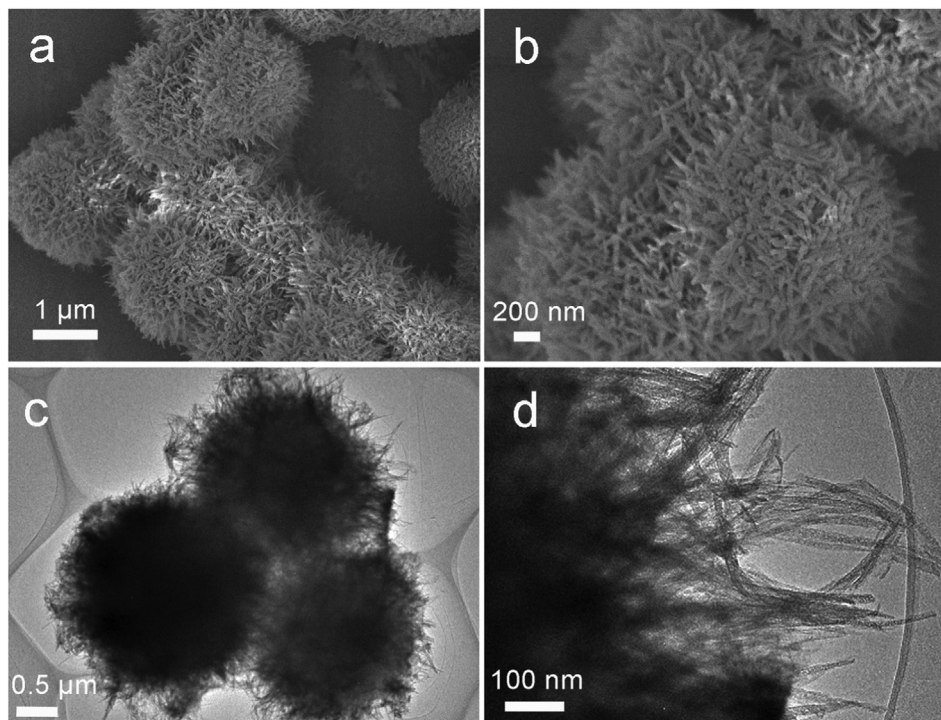
Fig. 4. FESEM (a, b) and TEM (c, d) images of the CS@Co$_2$CO$_3$(OH)$_2$ precursor.
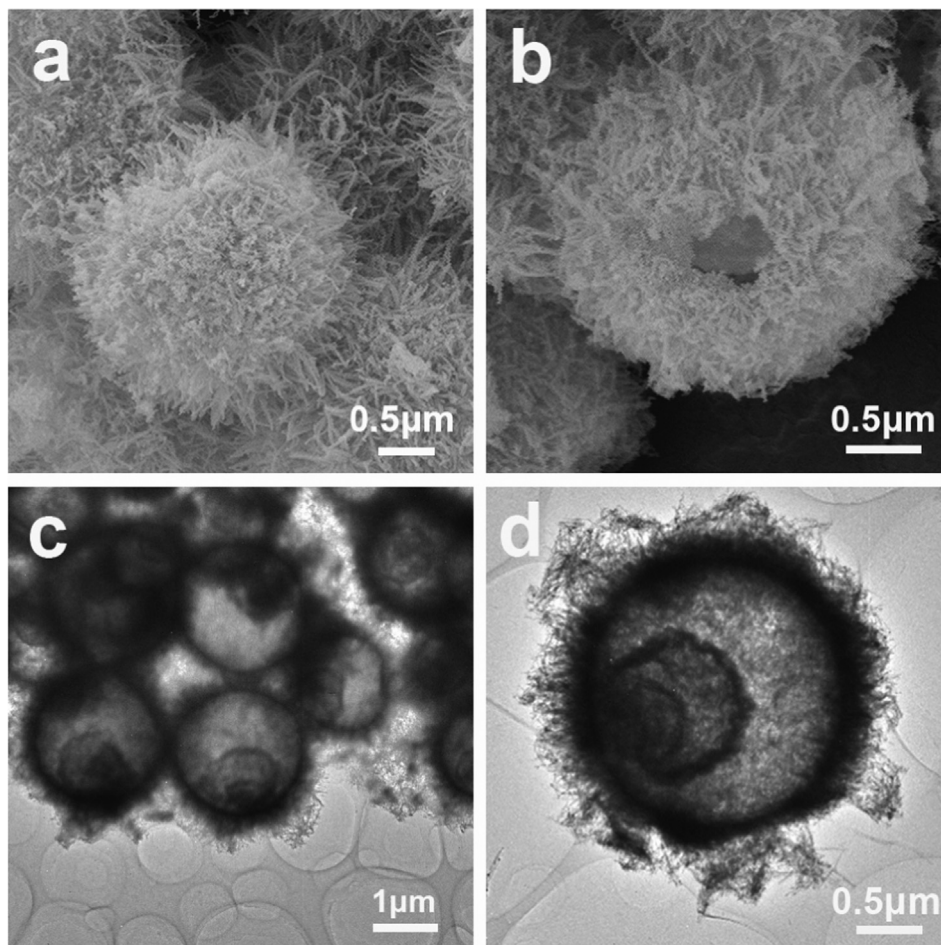

Fig. 5. FESEM (a, b) and TEM (c, d) images of the nanorod-assembled multi-shelled Co$_3$O$_4$ hollow microspheres.

microspheres is much less than the cobalt species on the exterior surface, so that the materials shrink into multi-shells during the gradual removal of the carbonaceous species. The multi-shelled Co_3O_4 hollow microspheres with well preserved nanorod-assembled exterior shell are thus prepared. The carbonaceous microspheres act as the multiple templates in the formation of multi-shelled hollow spheres [28]. The similar phenomenon is also reported for double-shelled Fe_2O_3 and triple-shelled NiO hollow spheres [17,29].

The electrochemical performance of the as-prepared multi-shell cobalt oxide (Co_3O_4) hollow microspheres as an electrode material for supercapacitors has been evaluated. Fig. 6a shows the cyclic voltammetry (CV) curves of the Co_3O_4 electrode at the scan rates of 2, 5, 10 and 50 mV s^{-1} respectively, in the voltage window between 0 and 0.5 V. It exhibits a distinct pair of broad redox peaks during the anodic and cathodic sweeps, which are typical characteristics of faradic redox reactions in the alkaline electrolyte. The possible redox reactions are based on Eqs. (2) and (3) [22]:
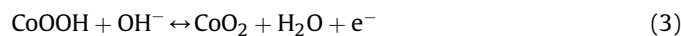
$$CoOOH + OH^- + H_2O \leftrightarrow 3CoOOH + e^- \qquad (2)$$

$$CoOOH + OH^- \leftrightarrow CoO_2 + H_2O + e^- \qquad (3)$$

Fig. 6b shows the galvanostatic charge and discharge curves at different current densities (2 A g^{-1}, 5 A g^{-1}, 10 A g^{-1}, 15 A g^{-1} and 20 A g^{-1}). Two plateaus are well observed on the discharge curves, which correspond to the two sequential redox reactions as described by Eqs (2) and (3). Fig. 6c shows the rate capability of the multi-shell Co_3O_4 hollow microspheres in the voltage range of 0−0.5 V. High specific capacitances of 394.4, 386, 360, 339, and 319 F g^{-1} can be delivered at the current densities of 2, 5, 10, 15 and 20 A g^{-1}, respectively. Fig. 6d shows the long-term cyclic stability of the Co_3O_4 electrode tested at the current density of 2 A g^{-1}. The

electrode can retain 92% of its original specific capacitance after 500 cycles. The capacitance is higher than many earlier reports for nanostructured Co_3O_4. For examples, Xia and coworkers reported the Co_3O_4 hollow microsphere had the high capacitances of 358 F g^{-1} at 2 A g^{-1} and 331 F g^{-1} at 10 A g^{-1} with the mass loading of 0.5 mg cm^{-2} in a three-electrode system. [22] The electrochemical performances are also superior to the flower-like Co_3O_4/C nanostructures [30] and the mesoporous crater-like Co_3O_4 microspheres with a mass loading of 2 mg cm^{-2} [31]. The results demonstrate the good advantages of multi-shell Co_3O_4 compared with the microspheres synthesized *via* template method or other cobalt−carbon composite materials with different structures. The superior electrochemical performance can be attributed to the multi-shelled hollow structures: (1) the smaller thickness of the interior shells than the exterior shell can enlarge the contact area between the electrode and electrolyte; (2) and the empty space between neighboring shells can provide easy electrolyte penetration path, ensuring the high utilization rate of the active material and the obtaining of high rate capability.

4. Conclusions

In summary, multi-shelled Co_3O_4 hollow microspheres are successfully synthesized with the assistance of carbon colloidal spheres as hard templates. Carbon spheres@cobalt−precursor (CS@Co−P) core−shell composite microspheres assembling from nanorods are facile prepared by a low-temperature hydrolysis route. The multi-shelled Co_3O_4 microspheres with complex interiors can be created after removing the carbon spheres by calcination in air. When evaluated as electrode material for supercapacitors, the multi-shelled Co_3O_4 microspheres exhibit high specific capacitance and superior rate capability. The remarkable electrochemical performance could be ascribed to the unique
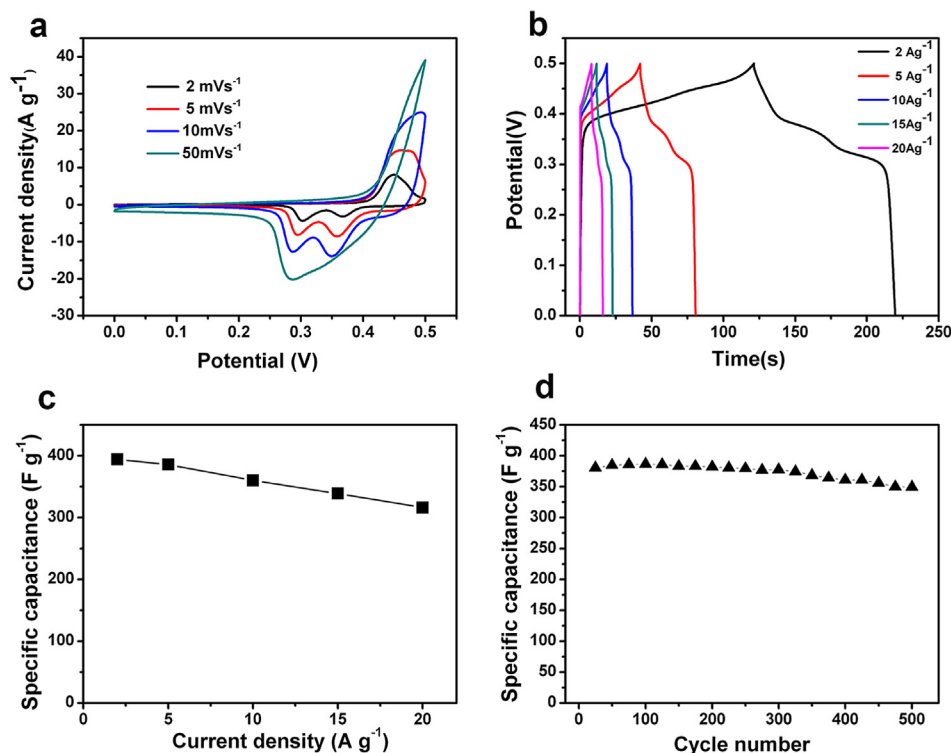

Fig. 6. (a) CV curves of Co_3O_4 microspheres at different scan rates; (b) charge and discharge curve and (c) corresponding specific capacitances at different discharge currents; (d) cycling performances of the Co_3O_4 microspheres at 2 A g^{-1}.

multi-shelled structures that facilitate the electrolyte penetration and provide more reactive sites for faradic reactions.

Acknowledgments

References

[1] Y.G. Sun, B.T. Mayers, Y.N. Xia, Nano Lett. 2 (2002) 481–485.
[2] Y.F. Zhu, J.L. Shi, W.H. Shen, X.P. Dong, J.W. Feng, M.L. Ruan, Y.S. Li, Angew. Chem. Int. Ed. 44 (2005) 5083–5087.
[3] J.H. Lee, Sens. Actuat. B Chem. 140 (2009) 319–336.
[4] W.Y. Li, L.N. Xu, J. Chen, Adv. Funct. Mater. 15 (2005) 851–857.
[5] X.W. Lou, L.A. Archer, Z.C. Yang, Adv. Mater. 20 (2008) 3987–4019.
[6] Z.Y. Wang, L. Zhou, X.W. Lou, Adv. Mater. 24 (2012) 1903–1911.
[7] J. Liu, S.Z. Qiao, J.S. Chen, X.W. Lou, X.R. Xing, G.Q. Lu, Chem. Commun. 47 (2011) 12578–12591.
[8] J. Liu, S.Z. Qiao, S.B. Hartono, G.Q. Lu, Angew. Chem. Int. Ed. 49 (2010) 4981–4985.
[9] H.C. Zeng, J. Mater. Chem. 21 (2011) 7511–7526.
[10] B. Liu, H.C. Zeng, Small 1 (2005) 566–571.
[11] Y.D. Yin, R.M. Rioux, C.K. Erdonmez, S. Hughes, G.A. Somorjai, A.P. Alivisatos, Science 304 (2004) 711–714.
[12] S.J. Ding, J.S. Chen, G.G. Qi, X.N. Duan, Z.Y. Wang, E.P. Giannelis, L.A. Archer, X.W. Lou, J. Am. Chem. Soc. 133 (2011) 21–23.
[13] H.X. Li, Z.F. Bian, J. Zhu, D.Q. Zhang, G.S. Li, Y.N. Huo, H. Li, Y.F. Lu, J. Am. Chem. Soc. 129 (2007) 8406–8407.
[14] S.A. Jenekhe, X.L. Chen, Science 283 (1999) 372–375.
[15] J.T. Zhang, J.F. Liu, Q. Peng, X. Wang, Y.D. Li, Chem. Mater. 18 (2006) 867–871.
[16] X.W. Lou, D. Deng, J.Y. Lee, L.A. Archer, Chem. Mater. 20 (2008) 6562–6566.
[17] X.Y. Lai, J. Li, B.A. Korgel, Z.H. Dong, Z.M. Li, F.B. Su, J.A. Du, D. Wang, Angew. Chem. Int. Ed. 50 (2011) 2738–2741.
[18] X.H. Xia, J.P. Tu, Y.J. Mai, X.L. Wang, C.D. Gu, X.B. Zhao, J. Mater. Chem. 21 (2011) 9319–9325.
[19] S.L. Xiong, C.Z. Yuan, M.F. Zhang, B.J. Xi, Y.T. Qian, Chem. Eur. J. 15 (2009) 5320–5326.
[20] C.Z. Yuan, L. Yang, L.R. Hou, L.F. Shen, X.G. Zhang, X.W. Lou, Energy Environ. Sci. 5 (2012) 7883–7887.
[21] B.R. Duan, Q. Cao, Electrochim. Acta 64 (2012) 154–161.
[22] X.H. Xia, J.P. Tu, X.L. Wang, C.D. Gu, X.B. Zhao, Chem. Commun. 47 (2011) 5786–5788.
[23] H.M. Du, L.F. Jiao, Q.H. Wang, J.Q. Yang, L.J. Guo, Y.C. Si, Y. Wang, H.T. Yuan, Nano Res. 6 (2013) 87–98.
[24] J.Y. Wang, N.L. Yang, H.J. Tang, Z.H. Dong, Q. Jin, M. Yang, D. Kisailus, H.J. Zhao, Z.Y. Tang, D. Wang, Angew. Chem. Int. Ed. 52 (2013) 6417–6420.
[25] X.M. Sun, Y.D. Li, Angew. Chem. Int. Ed. 43 (2004) 597–601.
[26] H.B. Wu, A.Q. Pan, H.H. Hng, X.W. Lou, Adv. Funct. Mater. 23 (2013) 5669–5674.
[27] J. Yang, H.F. Cheng, R.L. Frost, Spectrochim. Acta Part A Mol. Biomol. Spectrosc. 78 (2011) 420–428.
[28] X.Y. Lai, J.E. Halpert, D. Wang, Energy Environ. Sci. 5 (2012) 5604–5618.
[29] S.M. Xu, C.M. Hessel, H. Ren, R.B. Yu, Q. Jin, M. Yang, H.J. Zhao, D. Wang, Energy Environ. Sci. 7 (2014) 632–637.
[30] J.H. Jiang, W.D. Shi, S.Y. Song, Q.L. Hao, W.Q. Fan, X.F. Xia, X. Zhang, Q. Wang, C.B. Liu, D. Yan, J. Power Sources 248 (2014) 1281–1289.
[31] L. Wang, X.H. Liu, X. Wang, X.J. Yang, L.D. Lu, Curr. Appl. Phys. 10 (2010) 1422–1426.